# Potential Sites of PI-3 Kinase Function in the Endocytic Pathway Revealed by The PI-3 Kinase Inhibitor, Wortmannin

**Howard Shpetner, Marguerite Joly, David Hartley, and Silvia Corvera**

Program in Molecular Medicine and Department of Cell Biology, University of Massachusetts Medical School, Worcester, Massachusetts 01655

*Abstract.* Previously we have shown that PDGF receptor mutants that do not bind PI-3 kinase internalize after ligand binding, but fail to downregulate and degrade. To define further the role of PI-3 kinase in trafficking processes in mammalian cells, we have investigated the effects of a potent inhibitor of PI-3 kinase activity, wortmannin. At nanomolar concentrations, wortmannin inhibited both the transfer of PDGF receptors from peripheral compartments to juxtanuclear vesicles, and their subsequent degradation. In contrast, the delivery of soluble phase markers to lysosomes, assessed by the accumulation of Lucifer yellow (LY) in perinuclear vesicles after 120 min of incubation, was not blocked by wortmannin. Furthermore, wortmannin did not affect the rate of transferrin uptake, and caused only a small decrease in its rate of recycling. Thus, the effects of wortmannin on PDGFr trafficking are much more pronounced than its effects on other endocytic events. Unexpectedly, wortmannin also caused a striking effect on the morphology of endosomal compartments, marked by tubulation and enlargement of endosomes containing transferrin or LY. This effect was somewhat similar to that produced by brefeldin A, and was also blocked by pre-treatment of cells with aluminum fluoride ($AlF_4^-$). These results suggest two sites in the endocytic pathway where PI-3 kinase activity may be required: (*a*) to sort PDGF receptors from peripheral compartments to the lysosomal degradative pathway; and (*b*) to regulate the structure of endosomes containing lysosomally directed and recycling molecules. This latter function could be mediated through the activation of $AlF_4^-$-sensitive GTP-binding proteins downstream of PI-3 kinase.

PI-3 kinase was first discovered as an activity in immunoprecipitates of receptor and nonreceptor tyrosine kinases that phosphorylated the 3′ position of the inositol ring in PIns, PIns(4)P, and PIns(4,5)P2 (37). The association of this lipid kinase activity with receptors that stimulate cellular growth suggested a role for PI-3 kinase in mitogenic signaling (3). More recently, the existence of several biochemically distinct PI-3 kinases in mammalian cells has been reported (32, 33), and PI-3 kinase activity has been implicated in numerous cellular processes including membrane ruffling, chemotaxis, trafficking of membrane proteins, and activation of kinases such as protein kinase C (reviewed in reference 19). Thus, PI-3 kinases in mammalian cells have emerged as a diverse family of proteins that are likely to be involved in multiple essential cellular processes.

In yeast, deletions or mutations in the VPS34 gene, which encodes for the only detectable PI-3 kinase activity in these cells (31), lead to a dramatic alteration in the sorting of newly synthesized proteins to the yeast vacuole (13, 14, 31), and to a deficiency in the degradation of internalized α factor receptors (23). Thus, in yeast, PI-3 kinase regulates protein sorting events in the secretory and probably in the endocytic pathways. We have proposed that this sorting function of PI-3 kinase has been conserved in evolution, based on studies of mutant PDGF receptors impaired in PI-3 kinase binding, which are altered in postendocytic sorting to a degradative pathway (16, 17). The specific mechanism whereby PI-3 kinase activity is required for PDGF receptor trafficking is not known.

Recently it has been discovered that a potent fungal toxin, wortmannin, is a highly specific, potent inhibitor of the catalytic p110 subunit of mammalian PI-3 kinase (24, 40). Wortmannin rapidly and irreversibly inhibits PI-3 kinase catalytic activity in intact cells with an ID50 of 5–10 nM. At these concentrations, wortmannin does not inhibit any other known protein or lipid kinase activities in cells. The specificity and potency of wortmannin has made it a widely utilized tool to dissect the cellular functions of PI-3 kinase (5, 25). We have used wortmannin to explore further the role of PI-3 kinase on endocytic trafficking processes in mammalian cells.

Address all correspondence to S. Corvera, Program in Molecular Medicine and Department of Cell Biology, University of Massachusetts Medical School, 373 Plantation Street, Worcester, MA 01655. Tel.: (508) 856-6898. Fax: (508) 856-4289. E-mail: Scorvera@bangate1.ummed.edu

© The Rockefeller University Press, 0021-9525/96/02/595/11 $2.00

Here we show a comparative analysis of the effects of wortmannin on the trafficking of three markers of the endocytic pathway: transferrin, which internalizes and recycles through a well-characterized pathway involving sorting and recycling endosomes (15, 22), Lucifer yellow (LY),[1] a fluid phase marker which traffics to the lysosomal pathway, and the PDGF receptor (PDGFr), a transmembrane protein which normally does not recycle, but is instead delivered to the lysosome for degradation. The results presented here support the hypothesis that PI-3 kinase plays a critical role in the sorting of the PDGFr tyrosine kinase to the lysosomal pathway. Moreover, an unexpected role for PI-3 kinase in the control of membrane organelle structure is suggested by a dramatic effect of wortmannin on the morphology of endocytic organelles.

## Materials and Methods

### Cells

Human HepG2 cells transfected with human β-PDGF receptors (36), HeLa cells, and COS-7 cells were grown on glass coverslips or on 60 mm dishes to 80% confluence in DME supplemented with fetal calf serum (10%) (Upstate Biotechnology, Inc., Lake Placid, NY). In experiments involving fluid phase or transferrin uptake, cells were serum deprived for 2 or 18 h with no detectable difference in the results obtained. For experiments in which PDGFr internalization was analyzed, cells were serum starved for 18 h.

### Immunofluorescence

Cells were incubated at 37°C with PDGF-BB (20–50 ng/ml) (Upstate Biotechnology, Inc.) for the times indicated in each experiment. Cells were rapidly washed twice in ice-cold PBS, and fixed in 4% formaldehyde for 15 min at room temperature. Cells were washed four times with PBS, and permeabilized by immersion in methanol at −20°C for 6 min. Coverslips were briefly air dried, and stained with a monoclonal antibody raised against the receptor extracellular domain (PDGFR2; Oncogene Sciences, Mineola, NY), and goat antibodies to mouse IgG coupled to FITC or Rhodamine (Tago, Inc., Burlingame, CA). The fluid phase pathway was visualized by incubating cells with Lucifer yellow (5 mg/ml in DME) (Molecular Probes, Eugene, OR) for the times indicated. Cells were then fixed and permeabilized as described above, and the LY signal was enhanced by staining with an anti-LY polyclonal antibody (Molecular Probes) and goat antibodies to rabbit IgG coupled to FITC. The transferrin pathway was visualized by incubation of cells with Texas red–labeled transferrin (1 μg/ml in DME) (Molecular Probes), for the times indicated in each experiment, followed by fixation in 4% formaldehyde for 15 min at room temperature. Staining for βCOP and clathrin was done using rabbit antisera raised against βCOP (kindly provided by Dr. R. Klausner, NICHD, Bethesda, MD) or antisera raised against the COOH-terminal 15 amino acids of the clathrin heavy chain (18). Cells were mounted and visualized on a Zeiss IM-35 microscope, using a Nikon Apo 100/1.3 oil immersion lens. Data were recorded using a charge-coupled device (CCD) camera (Photometrics Ltd., Tucson, AZ) and visualized on a Silicon Graphics 4D/240 GTX. Where indicated, images were optically sectioned using digital imaging microscopy and a deconvolution algorithm that reverses the blurring introduced by the microscope optics (4). In these experiments, 20–30 serial two-dimensional images were recorded at 0.25-mm intervals using a thermoelectrically cooled CCD camera (Photometrics Ltd.). Each image was corrected for lamp intensity variations and photobleaching. Blurring of fluorescence from regions above and below the plane of focus was reversed using an iterative deconvolution algorithm based on the theory of ill-posed problems (4).

### Transferrin Uptake and Recycling

$^{125}$I-transferrin (31,000 cpm/μg) was prepared using 10 μg diferric transferrin (Boehringer-Mannheim Biochemicals, Indianapolis, IN) and Bolton Hunter reagent (Amersham, Arlington Heights, IL). To measure the rate of transferrin uptake, cells were grown to 80% confluence in 24-well multiwell dishes. Endogenous transferrin was removed by two sequential 40-min incubations in serum-free DME. Cells were then incubated in 500 μl of DME containing 0.2 μg/ml $^{125}$I-transferrin for the times indicated. Cells were washed four times in 1 ml of ice-cold PBS, and solubilized in 0.1% SDS. Radioactivity in the lysates was measured by gamma counting. Nonspecific uptake was determined in incubations containing nonlabeled transferrin (10 μg/ml). For the measurement of transferrin recycling, cells were incubated with 0.2 μg/ml $^{125}$I-transferrin for 60 min, and washed four times in ice-cold PBS. Recycling was initiated by adding DME at 37°C containing nonlabeled transferrin (10 μg/ml). At the times indicated monolayers were washed four times with 1 ml of ice-cold PBS, and solubilized in 0.1% SDS. Radioactivity in the lysates was measured by gamma counting.

### Measurement of Phosphoinositide Levels

Cells were grown in 100 mm dishes to 70–80% confluency, and labeled by incubation for 3 h at 37°C in Krebs-Ringer/Hepes buffer containing 2 mM sodium pyruvate, 2% BSA and 0.5 mCi/ml of [$^{32}$P]orthophosphate (New England Nuclear, Boston, MA). Cell monolayers were washed three times with ice-cold PBS, and rapidly scraped into 750 μl of MeOH/1 M HCl (1:1). Lipids were extracted with 400 μl of $CHCl_3$, deacylated, and analyzed by HPLC as described (1).

### Receptor Degradation

Cells were grown to 80% confluence in 60 mm culture dishes, and incubated for 18 h in serum-free, methionine-free DME containing [$^{35}$S]methionine (100 μCi/ml; Amersham) plus bovine serum albumin (1%), and then for 45 min in DME containing bovine serum albumin (1%) and methionine (0.3 mg/ml; DME-BSA). Cells were then incubated without or with PDGF-BB (50 ng/ml) (Upstate Biotechnology, Inc.) for 2 h. Where indicated, wortmannin, brefeldin A (BFA), or a mixture of both toxins was added 10 min before addition of PDGF. Cells were washed twice in ice-cold PBS, and lysed in 800 μl of a buffer containing 20 mM Tris (pH 8.0), 150 mM sodium chloride, 1% Triton X-100, 1% sodium deoxycholate, 0.1% SDS, 2 mM phenyl-methyl-sulfonyl fluoride, 1 mM benzamidine, 1 mM 1,10 phenanthroline, 10 μg/ml leupeptin, and 1 mM sodium vanadate (Sigma Chemical Co.). Receptors were immunoprecipitated with a polyclonal antibody to α- and β-PDGF receptors (Upstate Biotechnology, Inc.), resolved on 7.5% polyacrylamide gels, transferred to nitrocellulose, and exposed to autoradiographic film for 48 h.

### Effects of Wortmannin and BFA

Wortmannin (Sigma Chemical Co.) was dissolved in DMSO to a final concentration of 10 mM, dispensed into 5-μl aliquots and stored at −80°C. Wortmannin aliquots were thawed and diluted 1:1,000 in ice-cold PBS to a final concentration of 10 μM. Aliquots from this diluted stock were added directly to the cells to achieve the final concentrations indicated in each experiment. Because wortmannin is photosensitive and unstable in aqueous solutions, it was routinely thawed, diluted, and added to cells within 10 min. Thawed aliquots were discarded. BFA (Sigma Chemical Co.) was dissolved in ethanol to a final concentration of 50 mM. Aliquots from this stock were added directly to the cells to achieve the final concentration indicated in each experiment.

## Results

### Pathway of Internalization of Wild-type and Mutant PDGF Receptors

Previously we have found that PDGFr containing mutations which specifically impair PI-3 kinase binding can internalize, but fail to undergo down-regulation and degradation in response to PDGF (17). To better define the steps after internalization where PI-3 kinase is required for PDGFr down-regulation, we initiated studies to define the trafficking pathway of PDGFr from the cell surface to lysosomes. The intracellular localization of both wild-type

1. *Abbreviations used in this paper*: BFA, brefeldin A; LY, Lucifer yellow; PDGFr, PDGF receptor; Tf, transferrin; TR, Texas red.

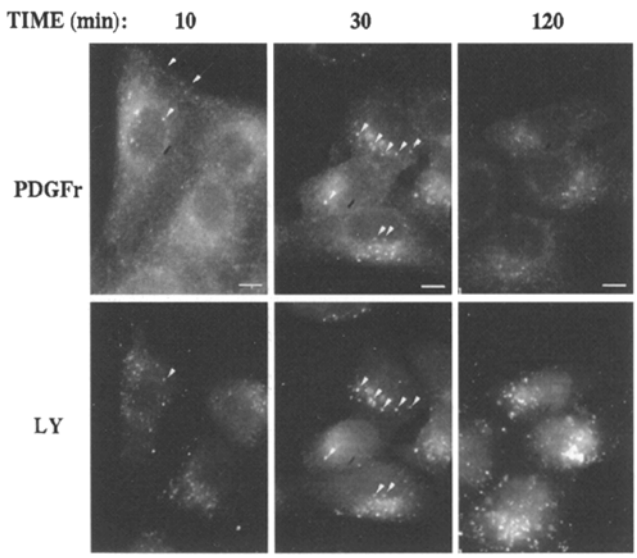


*Figure 1.* Internalization of PDGF receptors and LY. Cells were simultaneously exposed to PDGF (20 ng/ml) and to LY (5 mg/ml). After the indicated times of incubation at 37°C, cells were fixed, permeabilized, and stained for LY (*bottom*) and PDGF receptors (*top*) using specific polyclonal and monoclonal antibodies, respectively. Secondary antibodies labeled with FITC or rhodamine were used to detect the polyclonal or monoclonal antisera, respectively. Arrowheads point to vesicular structures labeled both with LY and PDGFr. Bars, 10 μm.

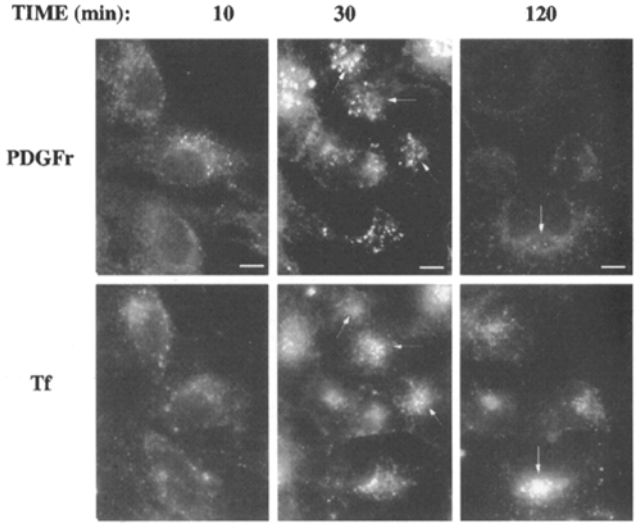


*Figure 2.* Internalization of PDGF receptors and transferrin. Cells were simultaneously exposed to PDGF (20 ng/ml) and Texas red–labeled transferrin (5 μg/ml). After the indicated times of incubation at 37°C, cells were washed, fixed, and stained with anti-PDGF receptor monoclonal antibodies, and FITC-coupled anti–mouse secondary antibodies. Despite the appearance of both transferrin and PDGF receptors in the same general vicinity (*arrows*), no precise co-localization was observed. Bars, 10 μm.

and mutant PDGFr was compared with that of LY, a lysosomally directed fluid phase marker (Figs. 1 and 3), and that of transferrin (Tf), a marker for a well-characterized recycling pathway (see Figs. 2 and 4).

HepG2 cells expressing wild-type receptors were exposed to PDGF and either LY (Fig. 1) or Tf (Fig. 2) at 37°C for the times indicated. Cells were fixed and processed for immunofluorescence as described in Materials and Methods. As early as 10 min after exposure of cells to PDGF, some colocalization of PDGFr and LY could be detected (Fig. 1, *left*). After 30 min, the PDGFr was found in larger, more perinuclear vesicles, and the co-localization with the fluid phase marker was very pronounced (Fig. 1, *middle*). After 120 min, much of the receptor signal disappeared due to lysosomal degradation, whereas the pericentriolar LY staining remained very intense (Fig. 1, *right*).

In contrast, at this level of resolution, a precise co-localization between the PDGFr and transferrin could not be detected at any time (Fig. 2). After 20–30 min of internalization, both PDGFr and transferrin were concentrated in a perinuclear region (Fig. 2, *middle* and *right*). However, transferrin was localized in more diffuse tubulo-vesicular structures which were clearly distinct from the larger vesicles containing PDGFr. These tubulo-vesicular elements probably correspond to the recycling endosome (15, 22). These results suggest that wild-type PDGFr molecules are sorted from recycling molecules relatively quickly (0–30 min) after internalization, but continue to co-localize with lysosomally destined fluid-phase markers (Fig. 1).

In marked contrast to the wild-type receptor, mutant receptors which lack PI-3 kinase binding sites (F40/51) remained at the cell periphery even after 30–90 min of incubation with PDGF (Fig. 3). These receptors were visualized in diffuse, peripheral structures, close to the plasma membrane (Fig. 3, *top*). In contrast to wild-type receptors (Fig. 1) the F40/51 mutant displayed little co-localization with LY (Fig. 3, *left*). Interestingly, although the F40/51 mutant recycles to the cell surface after internalization (17), the mutant displayed little co-localization with the pericentriolar transferrin (Fig. 3, *right*), suggesting that the recycling of PDGFr mutants to the cell surface takes place through a pathway that does not involve the transferrin recycling compartment. The peripheral localization of the receptor mutants, and their failure to co-localize with the bulk of the LY or Tf signals, suggest that receptors impaired in PI-3 kinase binding are arrested in their trafficking at an early step after endocytosis.

### *Effects of Wortmannin on PDGF Receptor and LY Trafficking*

To test further whether the differences between the trafficking pathways of wild-type and mutant PDGFr were due to differences in PI-3 kinase catalytic activity associated with the receptor cytoplasmic domain, we analyzed the effects of wortmannin, a potent and specific inhibitor of PI-3 kinase. Cells were incubated without or with wortmannin (50 nM) for 15 min, and then exposed to PDGF and LY. After 30 min of exposure of wortmannin-treated cells to PDGF, the receptor was found in a diffuse, peripheral localization (Fig. 4, *top right*), which contrasted markedly with the vesicular, pericentriolar localization of receptors in nontreated cells (Fig. 4, *top left*). Furthermore, the marked co-localization of PDGFr with LY (Fig. 4, *top* and *bottom left*) was lost in wortmannin-treated cells (Fig. 4, *top* and *bottom right*). These results are similar to those obtained studying PDGFr mutants impaired in PI-3 kinase

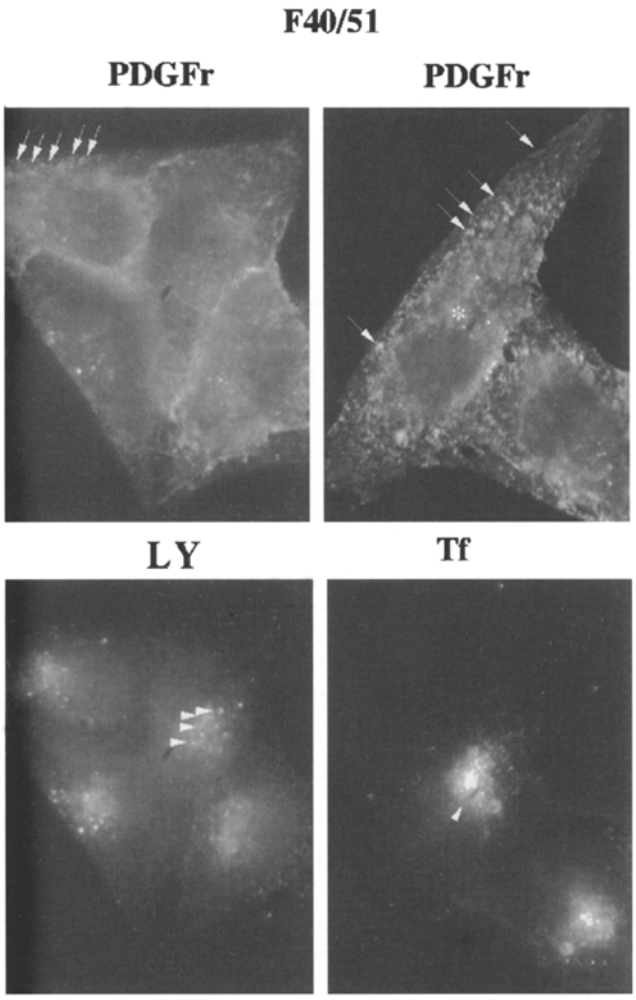


*Figure 3.* Internalization of F40/51 PDGF receptor mutants, LY, and transferrin. Cells expressing mutant (F40/51) receptors were incubated with PDGF and LY (*left*) or PDGF and transferrin (*right*) for 30 min at 37°C. Cells were fixed, and internalized molecules visualized as described in Figs. 1 and 2. Arrows point to the peripheral structures containing most of the mutant PDGFr (*top*). The asterisk in the top right panel was placed in the pericentriolar region containing the bulk of transferrin, to emphasize the lack of co-localization between PDGFr and the recycling endosome. Arrowheads point to internalized LY (*bottom left*) and transferrin (*bottom right*). Bars, 10 μm.

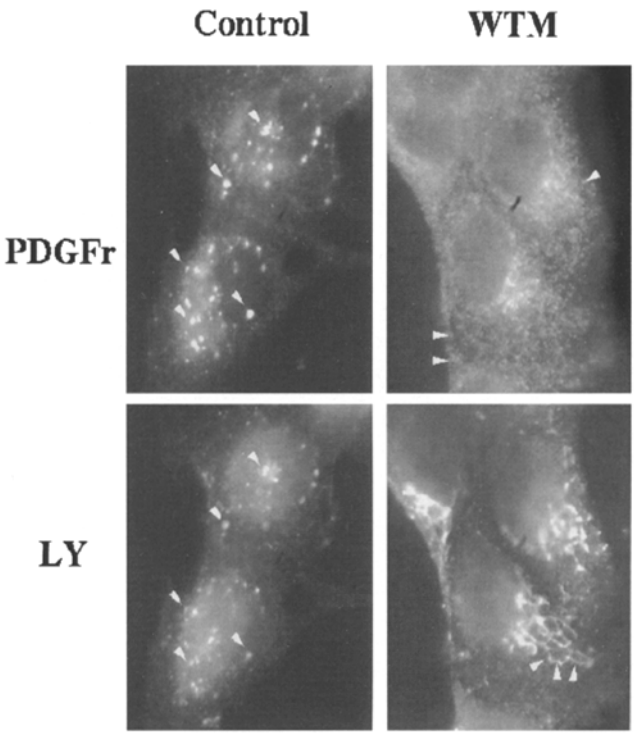


*Figure 4.* Effect of wortmannin on PDGF receptor and LY internalization. Cells were incubated without (*control*) or with (*WTM*) wortmannin (50 nM) for 10 min, and then exposed to PDGF and LY for 30 min. Cells were fixed, and internalized molecules visualized as described in Figs. 1 and 2. Note the precise co-localization of PDGFr and LY in the left panels (*arrowheads*), which is not apparent in wortmannin-treated cells in the right panels (*arrowheads*), and the appearance of interconnected tubules containing LY in response to wortmannin (*bottom right*).

binding (Fig. 3), and suggest that PI-3 kinase catalytic activity is required for PDGFr sorting from a specific peripheral compartment to later steps in the lysosomal pathway.

An unexpected finding in these studies was that, in addition to causing a retention of PDGFr in a peripheral compartment, treatment of cells with wortmannin caused a pronounced change in the morphology of endosomes containing LY (Fig. 4, *bottom right*). This morphological change consisted in the appearance of a tubulated network, which in many cells almost completely replaced the vesicular structures containing LY. In addition to the appearance of interconnected tubules, the amount of LY in wortmannin-treated cells appeared to be higher than that in untreated cells at early time points (Fig. 5, *bottom*). These alterations, however, did not appear to block the trafficking of LY to lysosomes, as a marked accumulation of the marker in large perinuclear vesicles was clearly visible after 120 min of incubation (Fig. 5, *extreme right*).

### *Effects of Wortmannin on the Transferrin Internalization Pathway*

To determine whether the morphological effect of wortmannin was restricted to endosomes labeled by LY, we analyzed the effects of the toxin on the transferrin pathway. Analysis of endosomes containing Texas red (TR)–transferrin in HepG2 cells, monkey COS-7 cells, and human Hela cells also revealed a pronounced effect of wortmannin on endosome morphology (Fig. 6). In nontreated cells TR–transferrin was distributed throughout the cell in a distinct punctate pattern, with an area of concentration in the juxtanuclear region which represents the recycling endosome (15, 22). In cells treated with wortmannin a striking increase in size, and decrease in number, of endosomes was observed (Fig. 6, *broken arrow*). Also apparent in many cells was the presence of fine tubules elongated from these enlarged endosomes (Fig. 6, *arrows*). The effect of wortmannin was observed at concentrations as low as 10 nM, and was maximal at 50 nM (not illustrated).

The effect of wortmannin occurred very rapidly, being detectable as early as 5 min after exposure of cells to the toxin (Fig. 7). After 20 min, a virtually complete transformation of endosomes containing transferrin (Fig. 7) or LY

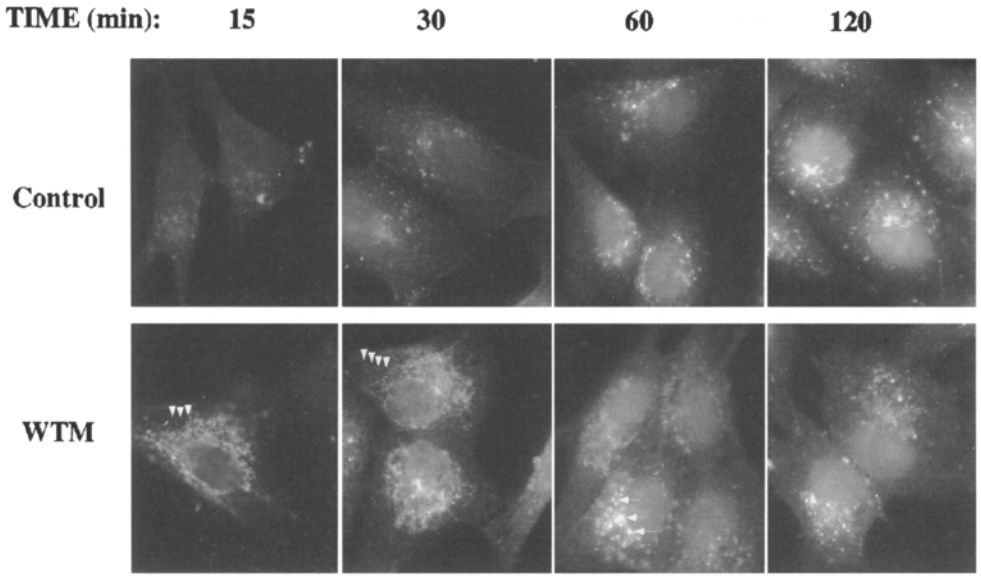


*Figure 5.* Effects of wortmannin on the internalization of LY. Cells were incubated without (*control*) or with (*WTM*) wortmannin (50 nM) for 10 min, and exposed to LY for the times shown. Cells were fixed and LY visualized as described in Fig. 1. Arrowheads are aligned along extended tubules, and arrows point to juxtanuclear vesicular structures apparent at later time points.

(not shown) into an interconnected tubular network was apparent in many cells. To determine whether the morphological changes induced by wortmannin would result in functional alterations in trafficking, we measured the rates of uptake and recycling of $^{125}$I-transferrin (Fig. 8). Treatment of cells with wortmannin had no detectable effect on the rate of accumulation of $^{125}$I-transferrin (Fig. 8, *left*). However, the rate of recycling was altered by wortmannin (Fig. 8, *right*). Whereas the rate of transferrin recycling measured in the first 10 min of the release assay appeared unaltered by wortmannin, the amount of transferrin released subsequent to 10 min appeared to be decreased by 30–40% in wortmannin-treated cells. After 40–50 min, however, all labeled transferrin was released from both untreated and wortmannin-treated cells. These results suggest that release of transferrin out of a specific compartment in the recycling pathway is slowed by wortmannin. Because the rates of transferrin and lipid recycling are similar (22), a decrease in transferrin recycling may reflect a general decrease in the rate of membrane flow out of early or recycling endosomes in response to wortmannin. This decrease could lead to the increased accumulation of LY and to the apparent enlargement of endosomes containing transferrin observed after treatment with the toxin (Figs. 5–7).

The inhibition of PDGFr trafficking and the changes in organelle morphology produced by wortmannin suggest that PI-3 kinase activity is required for at least two processes in the endocytic pathway: (*a*) to sort PDGFr out of a peripheral, postendocytic compartment into later steps in the endocytic pathway; and (*b*) to regulate both the kinetics of membrane flow and the morphology of endosomes containing lysosomally directed and recycling molecules.

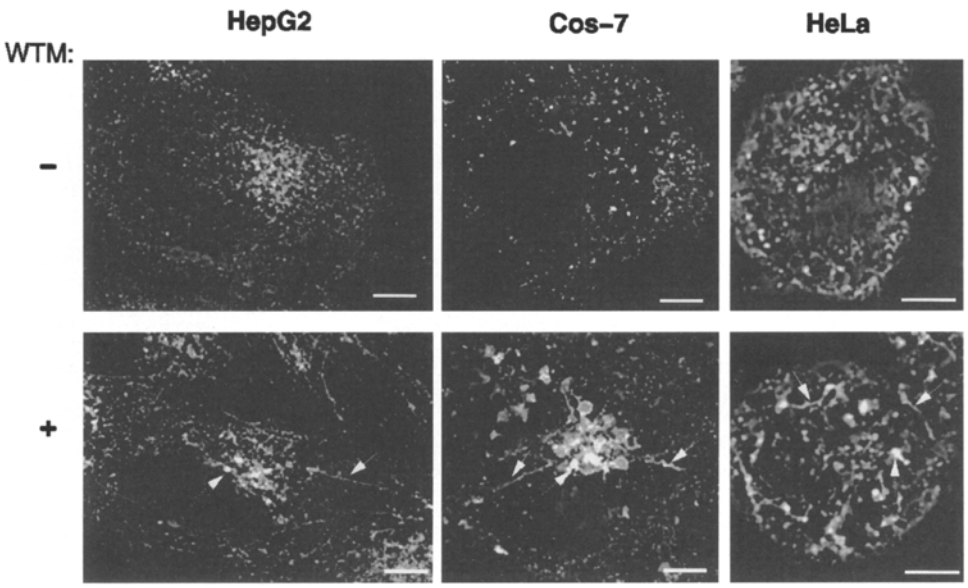


*Figure 6.* Effects of wortmannin on endosomes containing transferrin. HepG2, COS-7, and HeLa cells were incubated with Texas red–transferrin (5 μg/ml) for 30 min at 37°C. Wortmannin (*bottom*) was added to the medium to achieve a final concentration of 50 nM, and incubations were continued for a further 20 min. Cells were washed twice in ice-cold PBS, fixed in 4% formaldehyde, and visualized. Images comprise an individual optical section from the middle of the cell after restoration, as described in Materials and Methods. Arrowheads and arrows point to enlarged endosomes and tubulated structures found in wortmannin-treated cells. Bars, 10 μm.

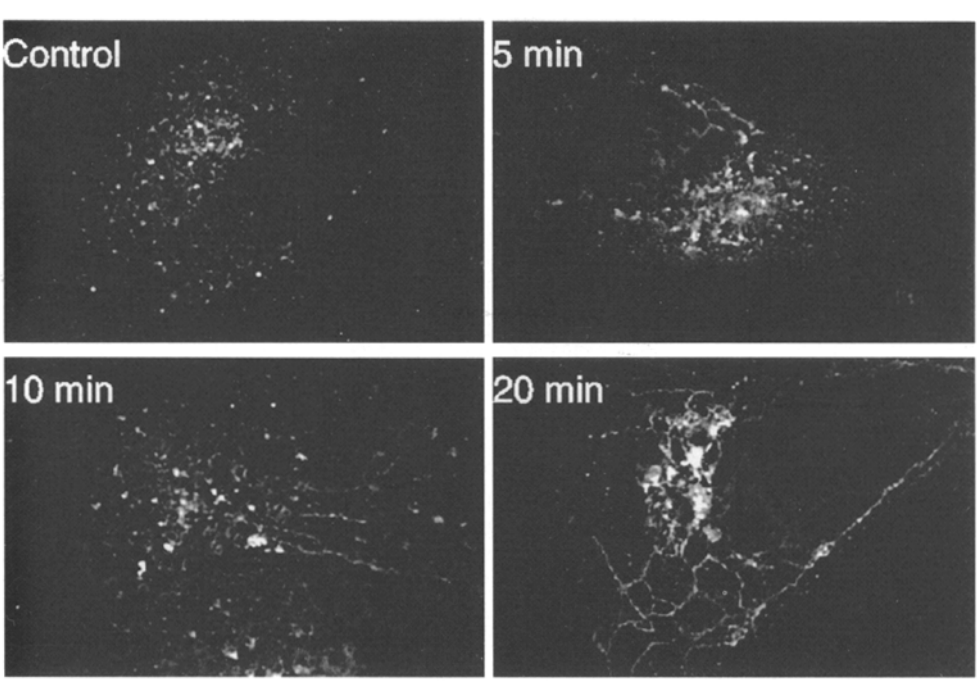


*Figure 7.* Time course of the effect of wortmannin on endosomes containing transferrin. HepG2 cells were incubated with TR-transferrin for 50 min at 37°C. Wortmannin (50 nM) was present for the last 5, 10, or 20 min of incubation as indicated. Cells were washed twice in ice-cold PBS, fixed in 4% formaldehyde, and visualized. Images are the sum of 20 individual optical sections comprising the middle of the cell after restoration, as described in Materials and Methods.

### *Effects of Wortmannin on Endogenous Phosphoinositide Levels*

An important question raised by these findings is whether specific phosphoinositide products of PI-3 kinases are involved in mediating both receptor sorting and organelle morphology in the endocytic pathway. To begin to address this question, we measured the levels of endogenous phosphoinositides in cells grown and treated exactly as described in the experiment shown in Fig. 7. Under these conditions, cells are exponentially growing, and are deprived of serum for only 2–3 h. The levels of endogenous phosphoinositides in these cells are shown in Table I. The most abundant 3′-phosphoinositide was PIns(3)P, which comprised ~75% of the total pool of 3′-phosphoinositides. Within 5 min of exposure of cells to 50 nM wortmannin, the levels of PIns(3)P decreased by 70%, but remained unchanged thereafter. In contrast, the levels of PIns(3,4,5)P3 decreased by 50% after 5 min of exposure to wortmannin, and were undetectable after 10 min of incubation with the toxin. Interestingly, the levels of PIns(3,4)P2 did not decrease in response to wortmannin. These results suggest that under conditions of exponential growth, 30% of cellular PIns(3)P, and most of the cellular pool of PIns(3,4)P2 are generated by wortmannin-insensitive PI-3 kinase/s.

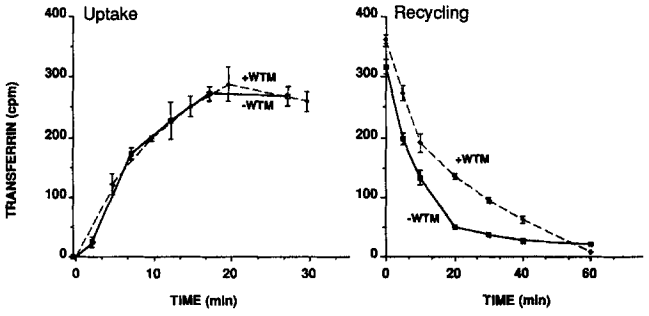


*Figure 8.* Effects of wortmannin on the internalization and recycling of transferrin. (*Left*) HepG2 cells were exposed to wortmannin (50 nM) for 10 min, and then to $^{125}$I-transferrin. Wortmannin (*WTM*) was present throughout the incubation. At the times indicated, cells were washed, and internalized radioactivity measured. (*Right*) Cells were incubated with $^{125}$I-transferrin for 60 min, and then exposed to wortmannin for 10 min. Cells were then washed three times with ice-cold PBS, and placed in media at 37°C containing excess unlabeled transferrin, in the absence or presence of wortmannin (*WTM*). After the times indicated, the radioactivity remaining associated with the cells was quantified. Plotted are the means ± SEM of three experiments performed in triplicate.

### *Similarities and Differences between the Effects of Wortmannin and BFA*

The tubulation of endosomes caused by wortmannin was reminiscent of the extensively reported effect of BFA (21, 38), which causes the extension of long, interconnected tu-

*Table I. Time Course of the Effects of Wortmannin on the Levels of Endogenous Phosphoinositides in Rapidly Growing HepG2 Cells*

| Time | PIns(3)P | PIns(3,4)P2 | PIns(3,4,5)P3 | PIns(4)P | PIns(4,5)P2 |
|---|---|---|---|---|---|
| *min* | | | | | |
| 0 | 13,053 | 2,706 | 1,172 | 527,060 | 1,027,909 |
| 5 | 4,517 | 5,560 | 570 | 452,303 | 977,197 |
| 10 | 4,533 | 3,102 | 0 | 537,946 | 1,021,332 |
| 20 | 4,732 | 5,101 | 0 | 478,838 | 1,063,518 |

Exponentially growing cells were labeled with [$^{32}$P]orthophosphate for 2 h as described in Materials and Methods, and treated with wortmannin (50 nM) for the times indicated. Monolayers were then scraped off the culture dishes, and lipids extracted, deacylated and separated by HPLC as described (1). The radioactivity in each deacylation product was expressed as total cpm/peak. The experiment was repeated twice with indentical qualitative results. Shown are the averaged raw values from these two independent experiments, which varied by ~20%.

bules from endocytic and secretory organelles. The mechanism whereby BFA elicits these morphological changes has been partially elucidated, and appears to involve an inhibition of cytosolic–coat assembly. We reasoned that a comparison of the effects of wortmannin and BFA on endocytic organelle structure and function might suggest mechanisms whereby wortmannin, and thus PI-3 kinase, function in the endocytic pathway. Therefore, we compared the effects of these toxins on cytosolic–coat protein assembly (Fig. 9), PDGFr trafficking (see Figs. 10 and 11), and endosome morphology (see Figs. 12 and 13).

To determine whether wortmannin, like BFA, would affect the assembly of known cytosolic coats, the distribution of βCOP, clathrin, and γ-adaptin were compared (Fig. 9). BFA blocked the assembly of coatomer, as evidenced by the change in the distribution of βCOP from a tightly concentrated juxtanuclear structure to a disperse distribution (Fig. 9, *middle*). BFA also blocked the assembly of γ-adaptin at the TGN (29), as evidenced by the loss of γ-adaptin and clathrin staining in a distinctly concentrated area next to the nucleus (Fig. 9, *bottom* and *top*). In contrast, wortmannin had no detectable effects on the distribution of clathrin, βCOP, or γ-adaptin (Fig. 9, compare columns *C* and *WTM*). Similar results were observed at concentrations of wortmannin up to 500 nM (not shown). These results indicate that unlike BFA, wortmannin does not inhibit the assembly of cytosolic coats in the secretory pathway. In addition, wortmannin had no effect on the ability of BFA to cause disassembly of coat components (not shown). Thus, the effects of wortmannin appear to be restricted to the endocytic pathway. One possible reason for this selectivity could be the presence, in the secretory pathway, of specific PI-3 kinase isoforms that are less sensitive to inhibition by wortmannin (reference 32; and Table I).

The effects of BFA and wortmannin on the subcellular localization and degradation of PDGFr were compared (Fig. 10). Cells were left untreated (Fig. 10, *top left* and *right*) or treated for 10 min with wortmannin (*bottom left*) or BFA (*bottom right*) and then exposed to PDGF (*top right* and *bottom*) for 60 min (Fig. 10). Both in the presence or absence of BFA receptors moved from the cell surface to large juxtanuclear vesicles (Fig. 10, *right*). Some tubulated structures containing PDGFr could be detected in BFA-treated cells (Fig. 10, *bottom right*), suggesting that, like other markers of the lysosomal pathway (39) PDGFr can exit the tubulated endosomal system induced by BFA. In contrast, in cells treated with wortmannin the movement of receptors from peripheral structures into pericentriolar vesicles was blocked (Fig. 10, *bottom left*). Addition of both toxins together blocked PDGFr movement to pericentriolar vesicles, indicating that BFA does not reverse the inhibitory effects of wortmannin on receptor trafficking (not shown). Furthermore, BFA had no significant effect on PDGF-induced receptor degradation (Fig. 11, *BFA*), whereas wortmannin fully inhibited this process (Fig. 11, *WTM*). Taken together, the results shown in Figs. 11 and 12 indicate that the alterations of organelle structure induced by BFA do not per se block PDGFr trafficking. Furthermore, these results suggest that the effects of wortmannin on organelle structure and PDGFr trafficking are independent.

The results shown above indicate two important differences between the effects of wortmannin and BFA; the effects of the former appear to be restricted to the endocytic pathway, and they also include an inhibition of PDGFr sorting probably resulting from inhibition of PI-3 kinase activity bound to the PDGFr cytoplasmic domain. Nevertheless, both wortmannin and BFA cause tubulation of or-

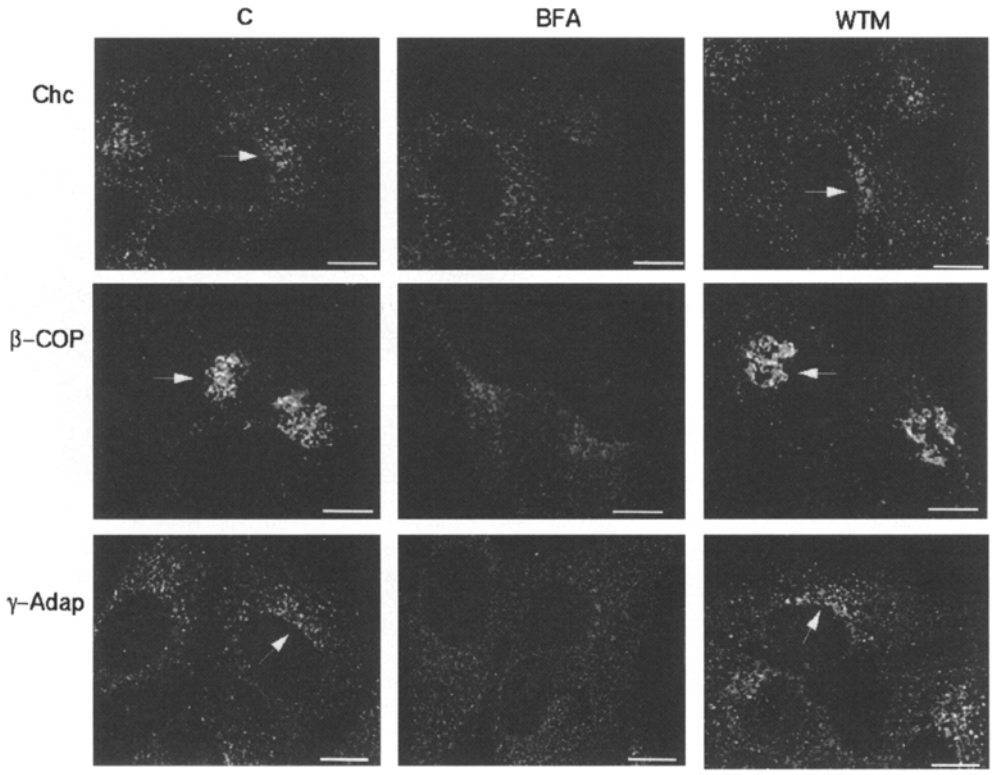


*Figure 9.* Effects of wortmannin and BFA on cytosolic coat distribution. HepG2 cells were treated with 10 μM BFA (*BFA*), 50 nM wortmannin (*WTM*), or nothing (*C*) for 10 min. Cells were fixed, permeabilized, and incubated with rabbit polyclonal antibodies against either the clathrin heavy chain (*Chc*) (*top*) or βCOP (*middle*) or with a mouse monoclonal antibody against γ-adaptin (*bottom*). Primary antibodies were detected with FITC-labeled secondary antibodies against rabbit or mouse immunoglobulins (Tago). Shown in each panel is one section through the middle of the cell after restoration. Bars, 15 μm.

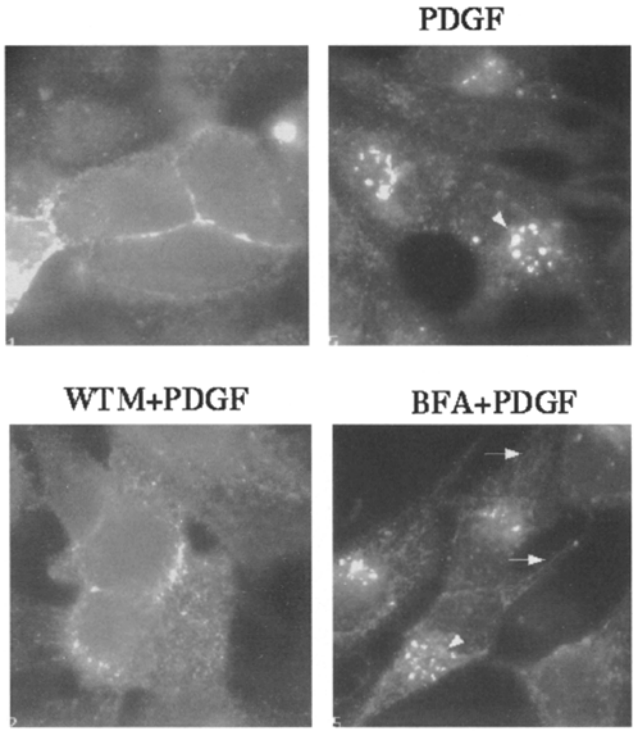


*Figure 10.* Effects of BFA and wortmannin on PDGF receptor distribution. HepG2 cells were treated with nothing (*top left*), 50 nM wortmannin (*bottom left*), 50 μM brefeldin-A (*bottom right*) for 10 min, and then exposed to PDGF (20 ng/ml) for 60 min at 25°C (*top right* and *bottom*). Cells were fixed, permeabilized, and stained with a monoclonal antibody against the PDGF receptor and anti–mouse immunoglobulins coupled to FITC. Arrowheads indicate juxtanuclear vesicles, and arrows indicate tubular structures containing PDGFr. Bars, 10 μm.

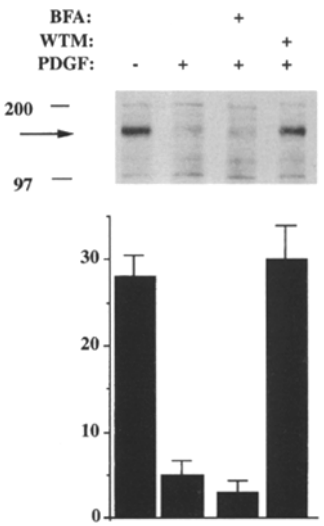


*Figure 11.* Effects of wortmannin and BFA on PDGF receptor degradation. HepG2 cells expressing the wild-type PDGF receptor were labeled with [$^{35}$S]methionine, and incubated for 2 h in the absence (−) or presence (+) of PDGF (50 ng/ml). BFA (*BFA*) (50 μM) or wortmannin (50 nM) were added 10 min before exposure to PDGF. Receptor immunoprecipitates were resolved on SDS-PAGE, and exposed to autoradiographic film. The expected position of the PDGF receptor is indicated with an arrow. Bars represent the means ± SEM of densitometric scans obtained from five independent experiments.

ganelles in the endocytic pathway. The effects of BFA have been shown to be blocked by $ALF_4$−, which inhibits the hydrolysis of GTP bound to ARF proteins, and results in a persistent activation of ARF and a concomitant stabilization of cytosolic coats on membranes (9, 21). To determine whether similar mechanisms might be involved in the effects of wortmannin and BFA on organelle morphology, we compared their sensitivity to $ALF_4$−.

Within 10 min of exposure of HepG2 cells to wortmannin or BFA, tubules containing transferrin could be observed (Fig. 12, *arrowheads*). The tubulated pattern induced by wortmannin was different from that of BFA in that condensation of endosomes was more pronounced, and tubules appeared to be shorter than those induced by BFA. However, the effects of both wortmannin and BFA were similarly blocked by pre-treatment of cells with $ALF_4$− (30 mM NaF + 50 μM $AlCl_3$). Similarly, the effect of wortmannin on endosomes containing LY was completely blocked by pre-treatment with $ALF_4$− (Fig. 13).

## Discussion

In this paper we have shown that wortmannin causes two distinguishable effects on trafficking in the endocytic pathway in mammalian cells. First, it appears to block the transit of activated PDGFr from a peripheral compartment to later steps in the lysosomal degradative pathway. This arrest in trafficking is also observed when PDGFr mutants impaired in PI-3 kinase binding are analyzed. Thus, it appears likely that the association of PI-3 kinase activity with the PDGFr cytoplasmic domain is necessary for its transit from a peripheral, early endocytic compartment into the lysosomal degradative pathway. Second, wortmannin causes a dramatic alteration in the morphology of endosomal elements containing transferrin and fluid phase markers. This latter effect is similar to that induced by the fungal toxin

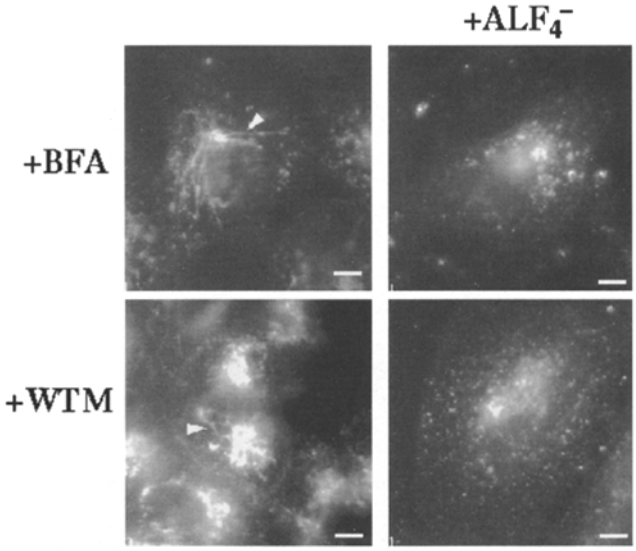


*Figure 12.* The effects of wortmannin and BFA on endosomes containing transferrin are blocked by $ALF_4$−. HepG2 cells were incubated with TR-transferrin for 30 min. $ALF_4$− (30 mM NaF + 50 μM $AlCl_3$) was then added (*+$ALF_4$−*), and incubations continued for 5 min. Wortmannin (*bottom*) or BFA (*top*) were then added at a final concentration of 50 nM or 50 μM, respectively. After an additional 20 min, cells were washed three times in ice-cold PBS, fixed in formaldehyde and visualized. Arrowheads indicate tubular structures, and arrows point to enlarged endosomes observed in response to wortmannin or BFA. Bars, 10 μM.

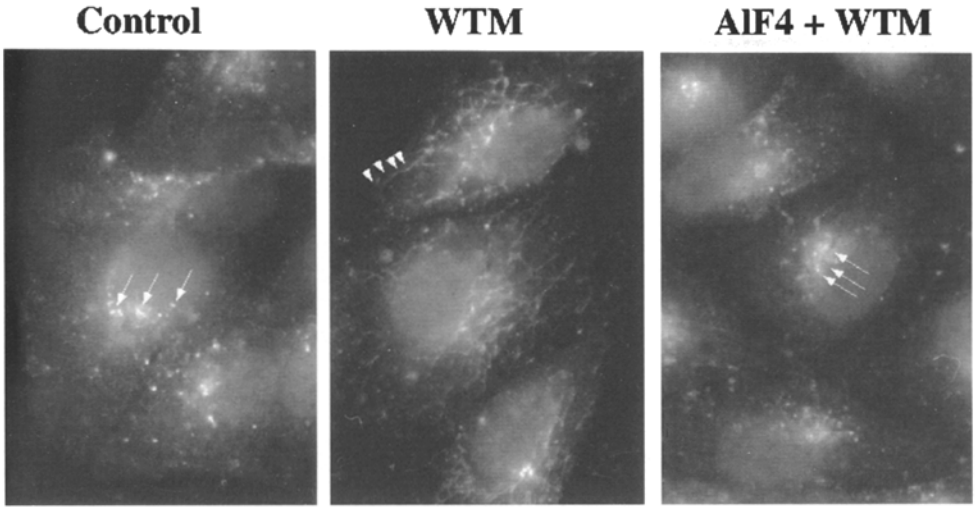


*Figure 13.* The effects of wortmannin on LY-containing endosomes are blocked by $ALF_4$–. Cells were incubated for 20 min with LY, and then for 5 min in the absence (*left* and *middle*) or presence (*right*) of $ALF_4$– (30 mM NaF + 50 μM $AlCl_3$). Wortmannin (*WTM*) (50 nM) was then added (*middle* and *right*), and after 15 min cells were fixed and stained as described above. Arrows point to vesicular structures containing LY, and arrowheads are aligned on tubulated structures which appear in response to wortmannin.

BFA, and can also be blocked by pre-treatment of cells with $ALF_4$–. These results suggest the hypothesis that $ALF_4$– sensitive GTP-binding proteins may operate downstream of PI-3 kinase.

### *Points in the Endocytic Pathway Where PI-3 Kinase Is Required for PDGFr Trafficking*

The high degree of co-localization of PDGFr and LY, and low degree of co-localization with transferrin shown in this study (Figs. 1 and 2) suggest that both PDGFr and fluid-phase molecules enter the sorting endosome, and are sorted together from recycling molecules. The mechanisms whereby activated wild-type PDGFr segregate from recycling molecules and maintain a co-localization with fluid phase markers is not known, but might involve its retention in the vesicular portion of the sorting endosome (10, 11, 22). Interestingly, however, in contrast to wild-type PDGFr, F40/51 mutant PDGFr remained dispersed in small structures at the cell periphery, and displayed little co-localization either with LY or with transferrin, which localized in more pericentriolar regions. Similarly, in cells treated with wortmannin wild-type PDGFr maintained a peripheral distribution, and lost the pronounced co-localization with LY observed in nontreated cells (Fig. 4). These results suggest that in the absence of PI-3 kinase activity, PDGFr trafficking is arrested at a very early step after internalization, before reaching the sorting endosome. The nature of the peripheral structures where PDGFr are arrested in the absence of PI-3 kinase is not known, but these structures did not display tubulation and enlargement in response to wortmannin (not shown), suggesting they are physically separate and functionally different from endosomes containing transferrin or Lucifer yellow, which tubulate in response to wortmannin. The results also support the hypothesis that the effect of wortmannin to block PDGFr sorting is independent of its effect on the structure of endosomes containing transferrin or LY.

### *Potential Mechanisms Involved in the Effects of Wortmannin on Organelle Morphology*

As with any other study involving the use of inhibitors, the possibility exists that this toxin may have direct targets other than PI-3 kinase. In our studies, we observed a close temporal correlation between the effects of wortmannin to decrease the endogenous levels of PIns(3)P (Table I) and to cause changes in organelle morphology (Fig. 7), as well as an identical dose-dependency for these effects (not illustrated). Wortmannin had no effect on the levels of PIns(4)P or PIns(4,5)P2, and at the concentrations used in these studies, wortmannin is not known to directly inhibit other protein or lipid kinases. Thus, the results presented here suggest, although they do not prove, that the effects of wortmannin on organelle morphology are indeed due to its inhibitory effect on PI-3 kinase activity.

Mammalian PI-3 kinases catalyze the formation of PIns(3)P, PIns(3,4)P2, and PIns(3,4,5)P3, but the specific physiological functions of each of these lipids are unknown. In our studies, low concentrations of wortmannin caused a rapid and pronounced decrease in endogenous PIns(3)P under conditions of exponential growth. A similar decrease in PIns(3)P occurs under conditions of serum starvation (Duckworth, B., and L. Cantley, unpublished results). Importantly, the effects of wortmannin on organelle structure are evident both in exponentially growing (Figs. 6 and 7) and in serum-deprived cells (Fig. 4 and data not shown). Because PIns(3)P is the only lipid detectable under both of these conditions (Table I; and reference 1), and it decreases in response to wortmannin with a time course that closely parallels the appearance of alterations in endosome morphology (compare Table I and Fig. 7), it is likely that PI-3 P is the lipid product of PI-3 kinase involved in the control of organelle structure.

PDGF internalization into the lysosomal pathway, which is analyzed in serum-starved cells, is closely paralleled by the appearance of PIns(3,4)P2 and PIns(3,4,5)P3, without a detectable increase in PIns(3)P (1). The appearance of both of PIns(3,4)P2 and PIns(3,4,5)P3 in response to PDGF is thought to result from the recruitment and stimulation of the p110/p85 PI-3 kinase isoform to the PDGF receptor cytoplasmic domain. This PI-3 kinase isoform is acutely sensitive to wortmannin, and in fact the PDGF-induced production of PIns(3,4)P2 and PIns(3,4,5)P3 is completely inhibited by wortmannin (Duckworth, B., and L. Cantley, personal communication). Thus, either or both

PIns(3,4)P2 and PIns(3,4,5)P3 could be involved in PDGFr sorting to the lysosomal pathway.

The similarity between the effects of wortmannin and BFA, consisting mainly in the formation of interconnected tubular networks (Figs. 6 and 7 and references 21 and 38), suggests that both toxins may affect similar targets. The targets of BFA appear to include activities that affect the exchange of GDP for GTP on ARF1, and thus the activation state of this protein (8, 12). Downstream cellular responses that are influenced by ARF1 are the binding of cytosolic–coat proteins like coatomer (20, 26) and γ-adaptin (29), as well as the activity of phospholipase-D (2, 6). It is thought that the changes in organelle morphology elicited by BFA result from the impaired binding of cytosolic–coat proteins. Although no specific cytosolic–coat proteins have been identified in endocytic vesicles, the phenotypic responses of these vesicles suggest that such endocytic cytosolic coats exist. Furthermore, isoforms of ARF or ARF-related GTP-binding proteins in the endocytic pathway may fulfill a function similar to that of ARF1 (7, 27, 30, 35).

The effects of wortmannin on endosomes suggest that this toxin may affect the assembly of cytosolic–coat components in the endocytic pathway. Furthermore, the findings that $AlF_4$- blocks these effects (Figs. 12 and 13) is consistent with the hypothesis that $ALF_4$--sensitive GTP binding proteins operate in the endocytic pathway, and that these may be regulated by PIns(3)P (Fig. 14). A role for phospholipids in the regulation of the activity of GTPases is consistent with recent reports which indicate a marked dependency on phosphoinositides for ARF1 exchange and GAP activities (34, 28).

An important difference between the effects of BFA and wortmannin is the specificity of wortmannin for organelles in the endocytic pathway. BFA causes tubulation of organelles both in the secretory and endocytic pathways, and the former effect is accompanied by inactivation of ARF1 and disassembly of Golgi-specific coats. The specificity of wortmannin for the endocytic pathway does not rule out the possibility that PI-3 kinase may operate both in the secretory and endocytic pathways to regulate coat assembly, as proposed in Fig. 14, because wortmannin does not completely deplete the endogenous levels of 3′-phosphoinositides. Table I indicates that a significant level of PIns(3)P remains in cells after treatment with wortmannin. This may represent the product of PI-3 kinases that are less sensitive to wortmannin, which have been previously described (32, 33), and which may be localized to the Golgi apparatus and/or other organelles in the secretory pathway.

In summary, the results shown here suggest that mammalian PI-3 kinases function at at least two steps in the endocytic pathway. First, PI-3 kinase activity appears to be required for the exit of internalized PDGFr from an early endocytic intermediate to sorting endosomes and later steps in the lysosomal degradative pathway. This process may require the localized synthesis of higher phosphorylated lipids PIns(3,4)P2 and PIns (3,4,5)P3, which appear upon association of the p85/p110 PI-3 kinase with the cytoplasmic domain of the PDGF receptor (1). A second, independent role of PI-3 kinase may be in maintaining the vesicular morphology of endosomes. It is likely that this function requires PIns(3)P, which is the most abundant 3′ phosphoinositide in cells, and is present both in exponentially growing and serum-deprived cells. Because it is likely that the maintenance of vesicular organelle morphology requires cytosolic–coat proteins and the activity of specific small GTP-binding proteins, our results suggest that downstream targets of PI-3 kinase products may include such cellular components.

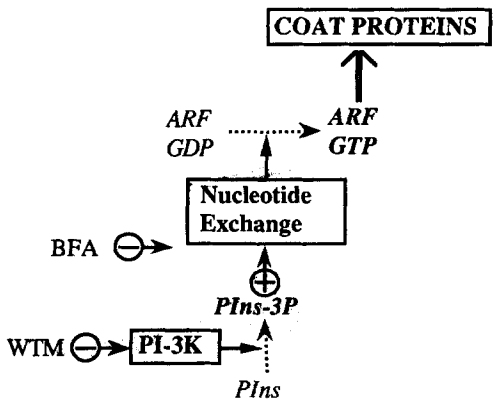


*Figure 14.* Potential targets for PI-3 kinase. Cytosolic coat-protein assembly on membranes is triggered by the activation of ARF GTPases by factors that catalyze nucleotide exchange. In our model, these factors are activated by PI-3 kinase products, for example PIns(3)P. The inhibition of PI-3 kinase activity by wortmannin results in a decrease in 3′-phosphoinositides, and thus to inhibition of nucleotide exchange. The process of nucleotide exchange is directly inhibited by BFA. The specificity of wortmannin for the endocytic pathway may result from the presence of PI-3 kinase activities that are less sensitive to the toxin which may be localized to the Golgi apparatus and other organelles in the secretory pathway.

We are very grateful to Drs. Brian Duckworth and Lucy Rameh from Dr. L. Cantley's Laboratory (Beth Israel Hospital, Boston, MA) for HPLC analysis of cellular phospholipids, and to L. Cantley for sharing unpublished results and for interesting and helpful discussions. We also wish to thank Mike Czech for his supportive and helpful comments, and for critical reading of this manuscript. Immunofluorescence studies were done using instrumentation and technical support from the Biomedical Imaging Group (Program in Molecular Medicine, University of Massachusetts Medical School).

This work was supported by National Institutes of Health grant DK-40330 to S. Corvera.

Received for publication 25 July 1995 and in revised form 1 November 1995.

### *References*

1. Auger, K., L. Serunian, S. Soltoff, P. Libby, and L. Cantley. 1989. PDGF-dependent tyrosine phosphorylation stimulates production of novel polyphosphoinositides in intact cells. *Cell.* 57:167–175.
2. Brown, H.A., S. Gutowski, C.R. Moomaw, C. Slaughter, and P.C. Sternweis. 1993. *Cell.* 75:1137–1144.
3. Cantley, L.C., K.R. Auger, C. Carpenter, B. Duckworth, A. Graziani, R. Kapeller, and S. Soltoff. 1991. Oncogenes and signal transduction. *Cell.* 64:281–302.
4. Carrington, W., K.E. Fogarty, and F.S. Fay. 1990. 3D fluorescence imaging of single cells using image restoration. *In* Non-Invasive Techniques in Cell Biology. K. Foster, editor. John Wiley-Liss, New York. 53–72.
5. Chung, J., T.C. Grammer, K.P. Lemon, A. Kazlauskas, and J. Blenis. 1994. PDGF- and insulin-dependent pp70$^{S6k}$ activation mediated by phosphatidylinositol-3-OH kinase. *Nature (Lond.).* 370:71–75.
6. Cockcroft, S., G.M.H. Thomas, A. Fensome, B. Geny, E. Cunningham, I.

Gout, I. Hiles, N.F. Totty, O. Truong, J.J. Hsuan. 1994. Phospholipase D: a downstream effector of ARF in granulocytes. *Science (Wash. DC).* 263: 523–526.

7. D'Souza-Schorey, C., G. Li, M.I. Colombo, and P.D. Stahl. 1995. A regulatory role for ARF6 in receptor-mediated endocytosis. *Science (Wash. DC).* 267:1175–1177.
8. Donaldson, J.G., D. Finazzi, and R.D. Klausner. 1992. Brefeldin-A inhibits Golgi membrane-catalyzed exchange of guanine-nucleotide onto ARF protein. *Nature (Lond.).* 360:350–352.
9. Finazzi, D., D. Cassel, J.G. Donaldson, and R.D. Klausner. 1994. Aluminum Fluoride acts on the reversibility of ARF1-dependent coat protein binding to Golgi membranes. *J. Biol. Chem.* 269:13325–13330.
10. Geuze, H.J., J.W. Slot, G.J.A.M. Strous, H.F. Lodish, and A.L. Schwartz. 1983. Intracellular site of asialoglycoprotein receptor-ligand uncoupling: double-label immunoelectron microscopy during receptor-mediated endocytosis. *Cell.* 32:277–287.
11. Geuze, H.J., J.W. Slot, G.J.A.M. Strous, J. Peppard, K. von Figura, A. Hasilik, and A.L. Schwartz. 1984. Intracellular receptor sorting during endocytosis: comparative immunoelectron microscopy of multiple receptors in rat liver. *Cell.* 37:195–204.
12. Helms, J.B., and J.E. Rothman. 1993. Inhibition by brefeldin-A of a Golgi membrane enzyme that catalyzes exchange of guanine nucleotide bound to ARF. *Nature (Lond.).* 360:352–354.
13. Herman, P., J. Stack, and S. Emr. 1992. An essential role for a protein and lipid kinase complex in secretory protein sorting. *Trends Cell Biol.* 2:363–368.
14. Hiles, I., M. Otsu, S. Volinia, M. Fry, I. Gout, R. Dhand, G. Panayotou, F. Ruiz-Larrea, A. Thompson, N. Totty, J.J. Hsuan, S. Courtneidge, P. Parker, and M. Waterfield. 1992. Phosphatidylinositol 3-kinase: structure and expression of the 110 kd catalytic subunit. *Cell.* 70:419–429.
15. Hopkins, C.R., A. Gibson, M. Shipman, D.K. Strickland, and I.S. Trowbridge. 1994. In migrating fibroblasts, recycling receptors are concentrated in narrow tubules in the pericentriolar area, and then routed to the plasma membrane of the leading lamella. *J. Cell Biol.* 125:1265–1274.
16. Joly, M., A. Kazlauskas, and S. Corvera. 1995. Phosphatidylinositol 3-kinase is required at a post-endocytic step in PDGF receptor trafficking. *J. Biol. Chem.* 270:13225–13230.
17. Joly, M., A. Kazlauskas, F. Fay, and S. Corvera. 1994. Disruption of PDGF receptor trafficking by mutation of its PI-3 kinase binding sites. *Science (Wash. DC).* 263:581–724.
18. Kapeller, R., R. Chakrabarti, L. Cantley, F. Fay, and S. Corvera. 1993. Internalization of activated PDGF receptor-phosphatidylinositol-3 kinase complexes: potential interactions with the microtubule cytoskeleton. *Mol. Cell. Biol.* 13:6052–6063.
19. Kapeller, R., and L. C. Cantley. 1994. Phosphatidylinositol 3-kinase. *BioEssays.* 16:565–576.
20. Klausner, R.D., J.G. Donaldson, and J.L. Schwartz. 1992. Brefeldin-A: insights into the control of membrane traffic and organelle structure. *J. Cell Biol.* 116:1071–1080.
21. Lippincott-Schwartz, J., L. Yuan, C. Tipper, M. Amherdt, L. Orci, and R.D. Klausner. 1991. Brefeldin A's effects on endosomes, lysosomes and the TGN suggest a general mechanism for regulating organelle structure and membrane traffic. *Cell.* 67:601–616.
22. Mayors, S., J.F. Presley, and R.R. Maxfield. 1993. Sorting of membrane components from endosomes and subsequent recycling to the cell surface occurs by a bulk-flow process. *J. Cell Biol.* 121:1257–1269.
23. Munn, A.L., and H. Riezman. 1994. Endocytosis is required for the growth of vacuolar $H^+$-ATPase-defective yeast: identification of six new *END* genes. *J. Cell Biol.* 127:373–386.
24. Okada, T., L. Sakuma, Y. Fukui, O. Hazeki, and M. Ui. 1994. Blockage of Chemotactic peptide-induced stimulation of neutrophils by wortmannin as a result of selective inhibition of phosphatidylinositol 3-kinase. *J. Biol. Chem.* 269:3563–3567.
25. Okada, T., Y. Kawano, T. Sakakibara, O. Hazeki, and M. Ui. 1994. Essential role of phosphatidylinositol 3-kinase in insulin-induced glucose transport and antilipolysis in rat adipocytes. *J. Biol. Chem.* 269:3568–3573.
26. Orci, L., D.J. Palmer, M. Amherdt, and J.E. Rothman. 1993. Coated vesicle assembly in the Golgi requires only coatomer and ARF proteins from the cytosol. *Nature (Lond.).* 364:732–734.
27. Peters, P.J., V.W. Hsu, C.E. Ooi, D. Finazzi, S.B. Teal, V. Oorschot, J.G. Donaldson, and R.D. Klausner. 1995. Overexpression of wild-type and mutant ARF1 and ARF6: Distinct perturbations of nonoverlapping membrane compartments. *J. Cell Biol.* 128:1003–1017.
28. Randazzo, P.A., and R.A. Kahn. 1994. GTP hydrolysis by ADP-ribosylation factor is dependent on both an ADP-ribosylation factor GTPase-activating protein and acidic phospholipids. *J. Biol. Chem.* 269:10758–10763.
29. Robinson, M.S., and T. Kreis. 1992. Recruitment of coat proteins onto Golgi membranes in intact and permeabilized cells: effects of brefeldin A and G protein activators. *Cell.* 69:129–138.
30. Shurmann, A., M. Breiner, W. Becker, C. Huppertz, H. Kainulainen, H. Kentrup, and H.G. Joost. 1994. Cloning of two novel ADP-ribosylation factor-like proteins and characterization of their differential expression in 3T3-L1 cells. *J. Biol. Chem.* 269:15683–15688.
31. Stack, J.H., and S.D. Emr. 1994. Vps34p required for yeast vacuolar protein sorting is a multiple specificity kinase that exhibits both protein kinase and phosphatidylinositol-specific PI-3 kinase activities. *J. Biol. Chem.* 269:31552–31562.
32. Stephens, L., F.T. Cooke, R. Walkers, T. Jackson, S. Volinia, I. Gout, M.D. Waterfield, and P.T. Hawkins. 1994. Characterization of a phosphatidylinositol-specific phosphoinositide-3-kinase from mammalian cells. *Curr. Biol.* 4:203–214.
33. Stephens, L., A. Smrcka, F.T. Cooke, T.R. Jackson, P.C. Sternweis, and P.T. Hawkins. 1994. A novel phosphoinositide-3-kinase activity in myeloid-derived cells is activated by G protein bg subunits. *Cell.* 77:83–93.
34. Tsai, S-C., R. Adamik, J. Moss, and M. Vaughan. 1994. Identification of a brefeldin-A insensitive guanine nucleotide-exchange protein for ADP-ribosylation factor in bovine brain. *Proc. Natl. Acad. Sci. USA.* 91:3063–3066.
35. Tsuchiya, M., S.R. Price, S.C. Tsai, J. Moss, and M. Vaughan. 1991. Molecular identification of ADP-ribosylation factor mRNAs and their expression in mammalian cells. *J. Biol. Chem.* 266:2772–2777.
36. Valius, M., and A. Kazlauskas. 1993. Phospholipase C-g1 and phosphatydylinositol-3 kinase are the downstream mediators of the PDGF receptor's mitogenic signal. *Cell.* 73:321–334.
37. Whitman, M., C.P. Downes, M. Keeler, T. Keller, and L. Cantley. 1988. Type I phosphatidylinositol kinase makes a novel inositol phospholipid, phosphatidylinositol-3-phosphate. *Nature (Lond.).* 332:644–646.
38. Wood, S.A., and W.J. Brown. 1992. The morphology, but not the function of endosomes and lysosomes is altered by brefeldin-A. *J. Cell Biol.* 119: 273–285.
39. Wood, S.A., J.E. Park, and W.J. Brown. 1991. Brefeldin-A causes a microtubule-mediated fusion of the trans-Golgi network and early endosomes. *Cell.* 67:591–600.
40. Yano, H., S. Nakanishi, K. Kimura, N. Hanai, Y. Saitoh, Y. Fukui, Y. Nonomura, and Y. Matsuda. 1993. Inhibition of histamine secretion by wortmannin through the blockade of phosphatidylinositol 3-kinase in RBL-2H3 cells. *J. Biol. Chem.* 268:25846–25856.